Nuclear Instruments and Methods in Physics Research B xxx (2017) xxx–xxx

Contents lists available at ScienceDirect

Nuclear Instruments and Methods in Physics Research B

journal homepage: www.elsevier.com/locate/nimb

Analysis of the response of PVA-GTA Fricke-gel dosimeters with clinical magnetic resonance imaging

Giorgio Collura [a,b,c], Salvatore Gallo [a,d], Luigi Tranchina [e], Boris Federico Abbate [f], Antonio Bartolotta [a], Francesco d'Errico [g,h,i], Maurizio Marrale [a,b,e,*]

[a] Dipartimento di Fisica e Chimica, Università degli Studi di Palermo, Palermo, Italy
[b] Istituto Nazionale di Fisica Nucleare (INFN), Sezione di Catania, Catania, Italy
[c] Dipartimento di Biopatologia e Biotecnologie Mediche, Università degli Studi di Palermo, Palermo, Italy
[d] Dipartimento di Fisica, Università degli Studi di Milano, Milano, Italy
[e] Advanced Technologies Network Center (ATeN Center), Università degli Studi di Palermo, Palermo, Italy
[f] U.O.C.-Fisica Sanitaria A.R.N.A.S. Ospedale Civico Palermo, Italy
[g] Scuola di Ingegneria, Università degli Studi di Pisa, Pisa, Italy
[h] Istituto Nazionale di Fisica Nucleare (INFN), Sezione di Pisa, Pisa, Italy
[i] Magnetic Resonance Research Center, Yale University School of Medicine, New Haven, CT, United States

ARTICLE INFO

Article history:
Received 10 April 2017
Received in revised form 8 June 2017
Accepted 13 June 2017
Available online xxxx

Keywords:
Gel dosimeter
Poly-vinyl alcohol
Glutaraldehyde
Magnetic resonance imaging
X-ray radiotherapy

ABSTRACT

Fricke gel dosimeters produced with a matrix of Poly-vinyl alcohol (PVA) cross-linked with glutaraldehyde (GTA) were analyzed with magnetic resonance imaging (MRI). Previous studies based on spectrophotometry showed valuable dosimetric features of these gels in terms of X-ray sensitivity and diffusion of the ferric ions produced after irradiation. In this study, MRI was performed on the gels at 1.5 T with a clinical scanner in order to optimize the acquisition parameters and obtain high contrast between irradiated and non-irradiated samples. The PVA gels were found to offer good linearity in the range of 0–10 Gy and a stable signal for several hours after irradiation. The sensitivity was about 40% higher compared to gels produced with agarose as gelling agent. The effect of xylenol orange (XO) on the MRI signal was also investigated: gel dosimeters made without XO show higher sensitivity to x-rays than those made with XO. The dosimetric accuracy of the 3D gels was investigated by comparing their MRI response to percentage depth dose and transversal dose profile measurements made with an ionization chamber in a water phantom. The comparison of PVA-GTA gels with and without XO showed that the chelating agent reduces the MRI sensitivity of the gels. Depth-dose and transversal dose profiles acquired by PVA-GTA gels without XO are more accurate and consistent with the ionization chamber data. However, diffusion effects hinder accurate measurements in the steep dose gradient regions and they should be further reduced by modifying the gel matrix and/or by minimizing the delay between irradiation and imaging.

1. Introduction

The increasing use of ionizing radiation in oncology requires appropriate dosimetric techniques. An accurate determination of the radiation dose delivered to the target tissue is critical for local tumor control [1] and a map of radiation doses in three dimensions is needed to verify the dose distributions generated by the treatment planning systems [2].

A large variety of dosimeters, such as ionization chambers [3,4], diamond [5,6] and silicon semiconductors [7,8], electron spin resonance (ESR) materials [9–32], thermoluminescent materials (TLDs) [33–40] and scintillators [41–43] can be employed for point measurements of X-ray doses. However, the above mentioned systems cannot map rapidly the radiation distributions around a target volume and cannot resolve high dose gradients.

Several chemical dosimeters are also available, such as radiochromic dyes [44] and films [45–48], acrylate monomers [49], emulsions of silver halides [50], and solutions containing ferrous ions [51–54]. The latter is one of the most common chemical dosimeters and consists of acidic oxygenated aqueous solutions

* Corresponding author at: Dipartimento di Fisica e Chimica, Università degli Studi di Palermo, Palermo, Italy.
E-mail address: maurizio.marrale@unipa.it (M. Marrale).

http://dx.doi.org/10.1016/j.nimb.2017.06.012
0168-583X/

of ferrous ions Fe^{2+}), which can be infused in gel matrices (Fricke Gels FG) [55,56]. Tissue equivalent phantoms can be produced with these gels, providing a 3D map of the dose delivered during radiation therapy [57]. These gels show excellent soft tissue equivalence also for of x-rays below 100 keV [58,59] which makes them interesting for diagnostic radiology applications.

Exposure of the gels to ionizing radiation induces a dose-dependent oxidation of ferrous (Fe^{2+}) to ferric ions (Fe^{3+}), which can be detected through optical tomography and/or magnetic resonance imaging (MRI) [57,60–62]. Indeed, the oxidation of ferrous ions also brings about a reduction of the longitudinal nuclear magnetic relaxation time T_1 [56] which can be measured by means of nuclear magnetic resonance (NMR) relaxometry and magnetic resonance imaging. MRI with clinical scanners offers non-destructive and inherently three-dimensional measurements with high spatial resolution [63]. In particular, T_1-weighted MRI sequences can effectively discriminate between regions with different absorbed dose [64–66]. Clinical MR scanners operating at 1.5 T have become the golden standard for gel imaging, since they are easy to find in hospitals. Therapeutic radiology departments are often close to diagnostic radiology departments, allowing local irradiation and imaging of the gels.

Unfortunately, Fricke gels present a significant shortcoming as they suffer from poor spatial stability of the signal due to diffusion of Fe^{3+} ions that restricts the time interval between irradiation and read-out [67]. Some reduction in the Fe^{3+} diffusion rates was achieved using different gelling agents, such as gelatin, agarose, and Sephadex, and adding chelating agents such as xylenol orange (XO) [68–70]. To date, the lowest ferric ion diffusion is that of the PVA-XO Fricke gel dosimeters proposed by Chu et al. [71], who reported a diffusion coefficient of 0.14 $mm^2\ h^{-1}$ at 20°C. The latter is about one order of magnitude lower than with conventional Fricke gels and about half of the value for agarose and gelatin gels with chelating agents [68]. However, PVA hydrogels were made with high concentrations of PVA (20% w/v) which causes an increase in viscosity over time (*e.g.*, days) at room temperature and an increase in optical scatter coefficient [71].

Recently, a new formulation of gels was introduced, made with 10% w/v of poly-vinyl alcohol and chemically cross-linked with glutaraldehyde (GTA) [72]. These gels show remarkable dosimetric features in terms of X-ray sensitivity and signal stability [72–74]. In this work, we further investigated the dosimetric features of these recent PVA–GTA gels with magnetic resonance imaging at 1.5 T. The dose response was measured and compared to that of agarose based gels. A comparative analysis was also done of the response in the presence or absence of the chelating agent xylenol orange, which is known to reduce the sensitivity of other gel formulations [75]. In all cases, the dosimetric accuracy of the 3D gels was investigated by comparing their MRI response to measurements made with an ionization chamber in a water phantom.

2. Materials and methods

2.1. Agarose gels preparation

Gels were prepared following the procedure described by Marrale *et al.* 2014 [66]. The gel solutions were prepared from a 3% w/w aqueous solution of agarose (Sigma–Aldrich®) with 25 mM Suprapure H_2SO_4 (96%) (Merck®), 1.5 mM ferrous ammonium sulphate hexahydrate (Mohr salt $[Fe(NH_4)_2(SO_4)_2{*}6H_2O]$ (Sigma–Aldrich®) and 0.165 mM xylenol orange-sodium salt $C_{31}H_{28}N_2Na_4O_{13}S$ (Sigma–Aldrich®). The 3% w/w agarose concentration gives us about 30 min to handle the formulations before it sets into a compact gel.

2.2. PVA-GTA gels preparation

The Fricke PVA-GTA gels were prepared following the procedure described by Marrale *et al.* 2017 [74]. The gels were prepared from a 10% w/v aqueous solution of hydrolyzed 99% purity Polyvinyl alcohol (PVA) with molecular weight between 85000 and 124000 (Sigma–Aldrich®), 1% w/v glutaraldehyde (GTA), 25 mM H_2SO_4 and 1.50 mM ferrous ammonium sulfate hexahydrate [$Fe(NH_4)_2(SO_4)_2{*}6H_2O$], 0.165 mM xylenol orange-sodium salt $C_{31}H_{28}N_2Na_4O_{13}S$. An additional batch of these gels was prepared without xylenol orange.

Ultrapure water (resistivity 18.6 $M\Omega{*}cm^{-1}$) was used in the preparation of both type of gels. The gels were then stored in the dark under refrigeration at 10 ± 1 °C, both after preparation and between irradiation and measurement, in order to minimize possible oxidation of Fe^{2+} ions induced by temperature or light.

2.3. Irradiation

For the dose response measurements, the gel samples were placed in CellStar® polypropylene tubes (Greiner Bio One International GmbH, Kremsmuenster, Austria) suitable for the subsequent MRI scans. The samples were irradiated up to 10 Gy with 6 MV X-rays from a Siemens Primus linear accelerator (LINAC) (Siemens Medical Systems CA, USA) at the ARNAS Ospedale Civico in Palermo (Italy). The samples were placed horizontally in a water phantom at the depth of maximum build-up (at about 1.5 cm from the surface) and irradiated within a 37×37 cm^2 field of x-rays.

Following the IAEA TRS-398 protocol (IAEA 2000) [76] reference X-ray dose values were measured using an ionization chamber (IC). The latter was a Semifex TW 31010 thimble ionization chamber (PTW, Freiburg GmbH, Germany) with a sensitive volume 0.125 cm^3, an active length 0.65 cm and a 0.55 cm inner diameter.

For the percentage depth dose (PDD) measurements, the gel samples were placed inside PMMA tubes parallel to the axis of a 10×10 cm^2 X-ray beam at a Source-to-Surface-Distance (SSD) of 100 cm (see Fig. 1A and B). In addition, transversal dose profiles for the 10×10 cm^2 field were measured at the depth of maximum build up along 20 cm. In this case as well, reference X-ray dose values were measured with the ionization chamber.

2.4. Instrumentation

All MRI scans of the samples were done between two and seven hours after irradiation. In particular, the scans of the depth and transversal dose profiles were done two hours after the irradiation. Before the scans, the samples were kept at room temperature for 30 min to thermalize. T_1–weighted magnetic resonance images were acquired on a 1.5 T Achieva scanner (Philips, Best, the Netherlands) using an eight channel head coil and an Inversion–Recovery sequence optimized for brain scans. The parameters set for the acquisitions were: echo time $T_E = 15$ ms, repetition time $T_R = 2500$ ms, number of acquisitions 2, voxel dimension $0.39 \times 0.39 \times 3.5$ mm^3 and matrix size 576 $\times$ 576 $pixel^2$. Data analysis was performed using in–house software developed in the Python language (Python Software Foundation, https://www.python.org/).

3. Results and discussion

3.1. Response as a function of dose

The response of Fricke gel dosimeters as a function of absorbed dose was analyzed by MRI. Previous MR studies suggested that only the longitudinal relaxation time is dose-dependent [66].

Please cite this article in press as: G. Collura et al., Analysis of the response of PVA-GTA Fricke-gel dosimeters with clinical magnetic resonance imaging, Nucl. Instr. Meth. B (2017), http://dx.doi.org/10.1016/j.nimb.2017.06.012

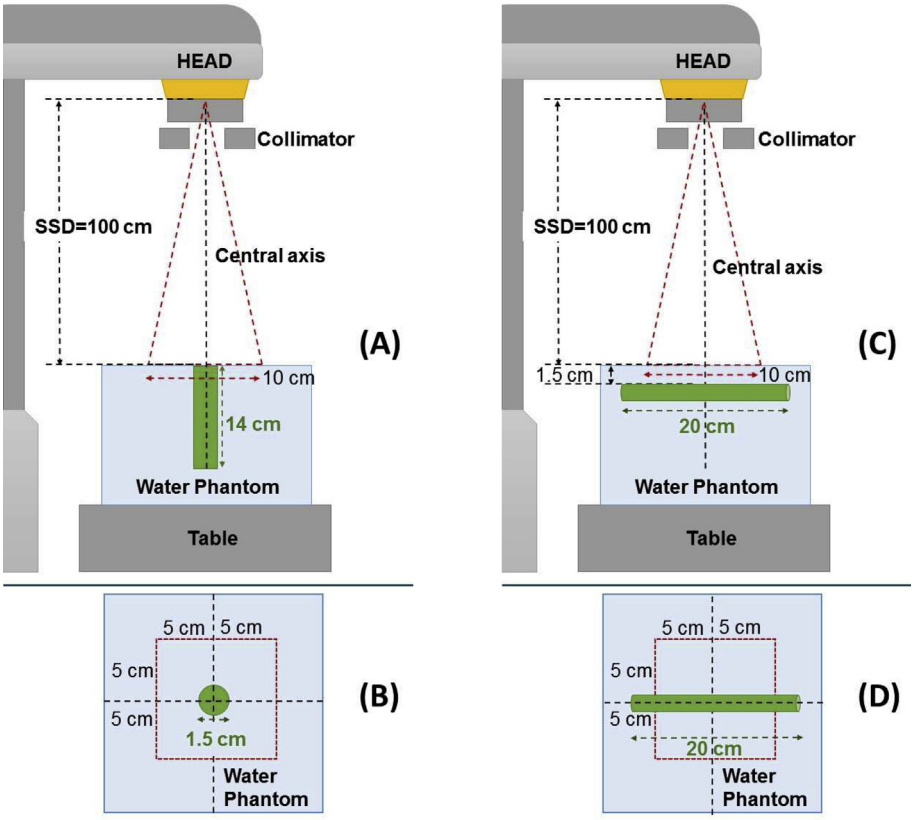

Fig. 1. (A) and (B) Lateral and top views of the irradiation setup used for the analysis of the percentage depth dose profile. (C) and (D) Lateral and top views for the irradiation setup used for the analysis of the trasversal dose profile.

Therefore, we focused on the longitudinal relaxation rate R_1, *i.e.* the reciprocal of the longitudinal nuclear relaxation time ($R_1 = 1/T_1$). The Fe^{3+} ions produced by radiation-induced oxidation of Fe^{2+} ions act as T_1-contrast agents, making the longitudinal relaxation of H-proton magnetization faster. As a consequence, R_1 is an increasing function of dose. As dose increases, the MRI signal from Inversion-Recovery sequences tends to saturate at lower values of T_I. Therefore, a reduction of the longitudinal relaxation time T_1 is observed with the consequent increase of the MRI signal.

At first, we determined the response to X-rays of PVA-GTA Fricke gels containing xylenol orange. Fig. 2 shows the dose dependent MRI signal drawn from central regions of interest (ROI) of our gel samples. The experimental data were fitted with a linear curve according to Eq. 1:

$$MR_{SIGNAL} = m \times DOSE + q \quad (1)$$

where m and q are the slope and intercept of the linear regression, respectively. The m value represents the sensitivity to the X-ray doses.

The correlation coefficient reported in Table 1 confirms that the MRI signal increases linearly with dose in a dose-range of clinical relevance.

In line with our previous work on agarose gels [65], our first measurements illustrated in Fig. 2 were done with an Inversion Time (T_I) of 400 ms. In order to optimize the read out of PVA-GTA gels, we did an analysis of the dependence of the MRI sensitivity on T_I, i.e. the slope of the MRI response *vs* dose. The T_I values tried in this analysis ranged between 250 ms and 600 ms.

As can be seen in Fig. 3 the sensitivity peaks for T_I values of 400 ms. Therefore, in order to maximize the dose dependent response, we used a value of T_I equal to 400 ms in all other measurements reported in this work.

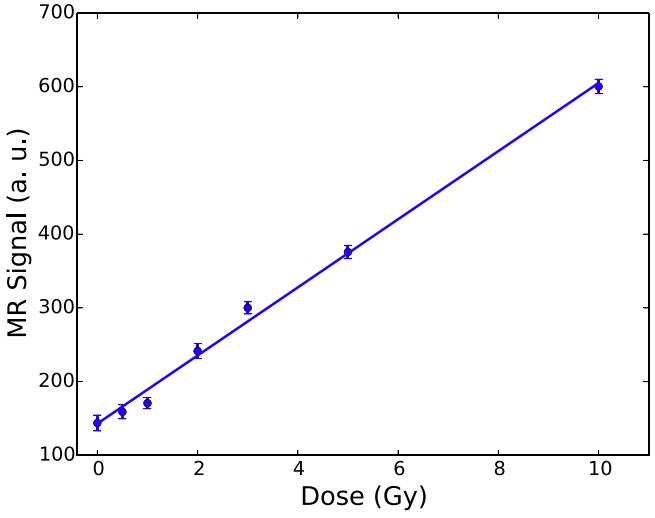

Fig. 2. MRI response of PVA-GTA Fricke gel with xylenol orange as a function of dose. Error bars correspond to 1 S.D.

Table 1
Parameters (±1 S.D.) of the best fit procedure on the calibration curves.

Gel matrix	Intercept	Slope	r^2
PVA-GTA-XO	143 ± 7	46.2 ± 1.6	0.995
Agarose-XO	42 ± 5	33.3 ± 1.2	0.995
PVA-GTA	45 ± 26	173 ± 7	0.995

Please cite this article in press as: G. Collura et al., Analysis of the response of PVA-GTA Fricke-gel dosimeters with clinical magnetic resonance imaging, Nucl. Instr. Meth. B (2017), http://dx.doi.org/10.1016/j.nimb.2017.06.012

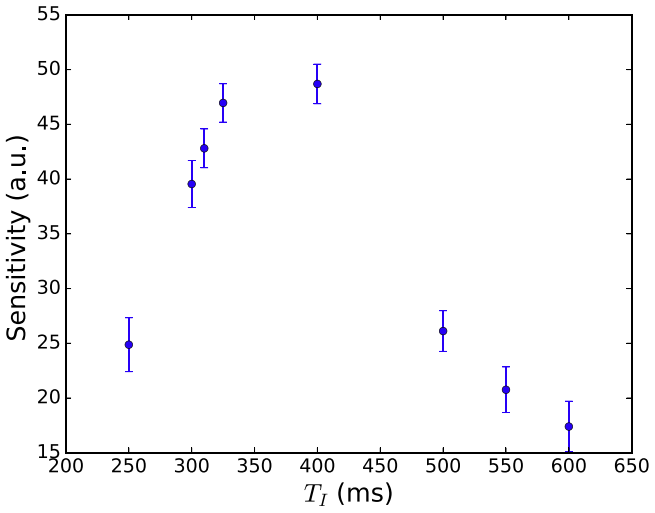

Fig. 3. Dependence of sensitivity of PVA-GTA Fricke gel with xylenol orange on the inversion time T_I. Error bars correspond to 1 S.D.

3.2. Comparison of PVA with agarose gels

An extensive comparative analysis of the new PVA-GTA gels was performed with respect to the agarose dosimeters that had been thoroughly investigated in previous studies [67,60,65,66]. Fig. 4 shows the MRI response of agarose and PVA-GTA gels both containing xylenol orange.

As shown in Fig. 4 and Table 1, the sensitivity of the PVA-GTA gels is about 40% higher than that of agarose gels. In addition, these new gels show a very low diffusion of Fe^{3+} ions [73,72,74]. This suggests that the gel matrix plays a decisive role in the oxidation of ferrous Fe^{2+} ions into Fe^{3+} ions as well as in the interaction between hydrogen nuclei and the lattice, affecting the relaxation rate R_1 and making the PVA-GTA gels more sensitive than agarose gels.

3.3. Analysis of the effect of xylenol orange

A further aspect of our study was the investigation of the effects of xylenol orange on the MR signal. The use of xylenol orange in agarose Fricke gels helps reduce diffusion effects and also allows optical analyses; however, XO also introduces a significant decrease of the MRI signal and longitudinal relaxation rate R_1 [75]. In order to clarify whether the effect also occurs for PVA-GTA gels, we performed experiments on samples prepared with and without xylenol orange. The results of these analyses are reported in Fig. 5 and Table 1.

Fricke gels prepared without XO show a higher sensitivity to X-rays than gels with XO. In particular, best fit functions obtained for these dosimetric gels show a slope over three times higher compared to gels with XO (Table 1). Xylenol orange binds to ferrous ions and becomes part of the lattice of the gel. In the presence of XO a given dose produces a lower intensity signal, thus XO either reduces the effect of oxidation of ferrous ions or otherwise hinders the exchange of energy between the spin and the lattice slowing longitudinal relaxation, as also reported in the literature [75].

3.4. Stability of the MR sensitivity after irradiation

The stability of the NMR signal over time after irradiation was also investigated. For the purpose, samples with and without XO were read from 2 h up to 7 h after irradiation. Fig. 6 shows the

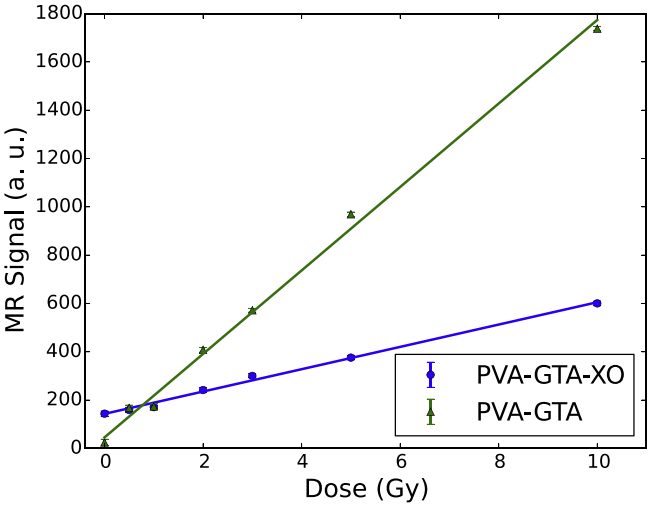

Fig. 5. Comparison of the MR response of Fricke PVA-GTA gels with and without xylenol orange. Error bars correspond to 1 S.D.

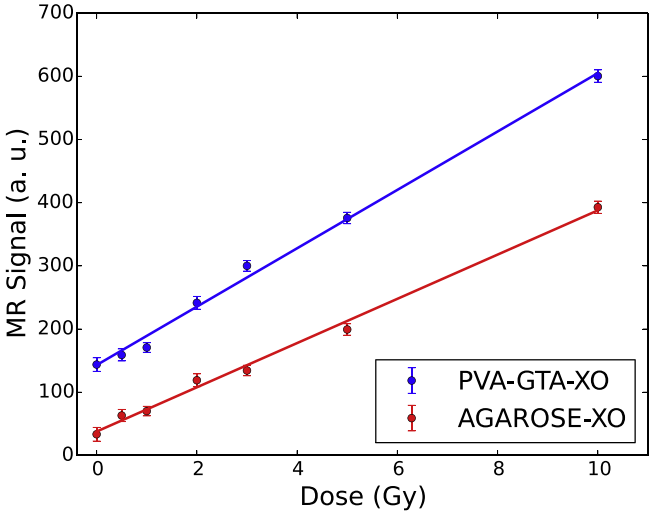

Fig. 4. Comparison of the MRI response of PVA-GTA and agarose gels. Error bars correspond to 1 S.D.

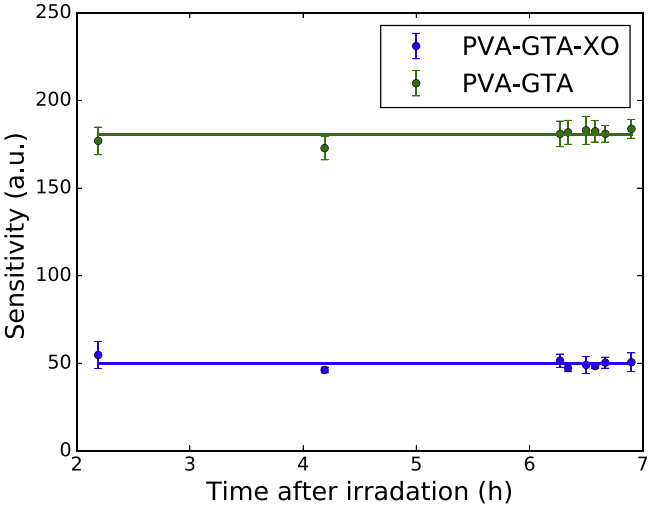

Fig. 6. Stability of sensitivity of Fricke xylenol gel dose response after irradiation. Error bars correspond to 1 S.D.

Please cite this article in press as: G. Collura et al., Analysis of the response of PVA-GTA Fricke-gel dosimeters with clinical magnetic resonance imaging, Nucl. Instr. Meth. B (2017), http://dx.doi.org/10.1016/j.nimb.2017.06.012

evolution of the sensitivity (calculated as the slope of the calibration curves 1) as a function of time after irradiation.

PVA-GTA gels with and without XO display an MR signal that is stable in the time interval we analyzed. We chose an interval of 7 h as it appears to be a realistic time frame for the scan of the gels after irradiation.

3.5. First dose mapping tests

A final aspect of this study was the acquisition of one-dimensional dose profiles with cylindrical gel rods immersed in a water phantom. With these gel rods, we acquired depth dose profiles along the beam axis of a 10×10 cm^2 field of 6 MV X-rays, as well as transversal dose profiles across the field, at the depth of maximum buildup.

For the determination of the axial and transversal dose profiles, two sets of 20 cm long, 1.5 cm diameter, gel tubes were prepared, filled with PVA-GTA Fricke gels manufactured with and without XO. A photograph of the tubes is shown in Fig. 7. MR images of the irradiated tubes are also shown in Fig. 7b, where the tube on the left contains PVA-GTA gel with XO and the tube on the right contains PVA-GTA gel without XO. Clearly, the signal is higher in the gels without XO, as expected from our previous dose response measurements. As in the dose response analysis, the MRI signal was taken from central ROIs of the samples and was plotted as a function the distance from the center of the radiation field. In order to assess the dosimetric accuracy of the gels, the MR data were plotted against dose values acquired with our ionization chamber in the water phantom.

In the transversal dose measurements, gels produced without XO are able to map quite accurately the central part of the dose profile as well as the lateral tails. The gel response without XO is quite different: in fact, the profiles orthogonal to the beam axis are more accurate and consistent with the data from the ionization chamber. Indeed, as shown in Fig. 8, the presence of XO reduces the sensitivity of the dosimetric gels by a factor of three and makes the images much noisier. Therefore, although the presence of XO can help reduce the diffusion of ferric ions, its use may not always be optimal for MR imaging. However, both gel types clearly show diffusion effects compared to the IC readings in the dose gradients at the edges of the X-ray field. This is consistent with the fact that the MRI scans were done 2 h after the irradiations, which leads to a spreading of the signal in the order of millimeters, even when gels contain XO.

These considerations also apply to the depth dose profiles measured along the X-ray beam axis using PVA-GTA gels with and without XO. Quantitative data were derived by taking the MR signal from central ROIs of the tubes, at different depths along the X-ray beam. Results are reported in Fig. 9, showing that gels without XO can map the IC dose profile more accurately both in the initial dose gradient, at depths smaller than the build-up, and at higher depths. Conversely, the response of gels with XO is noisy and the signal fluctuations obscure the expected trends.

The two types of PVA-GTA gels, with and without XO, presented different degrees of accuracy, due to their different sensitivity and

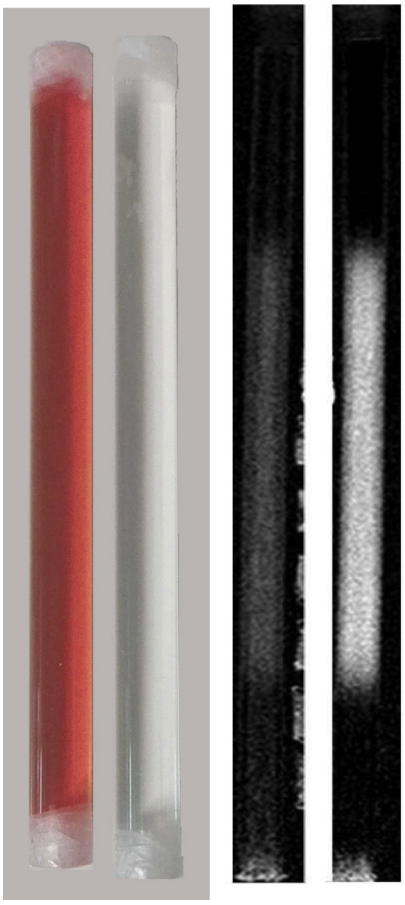

(a) (b)

Fig. 7. (a) Picture of the PMMA tubes filled with PVA-GTA gel with XO (left) and without XO (right) used for dose profile analysis. (b) Lateral dose profiles measured by means of PVA-GTA gels with XO (left) and without XO (right).

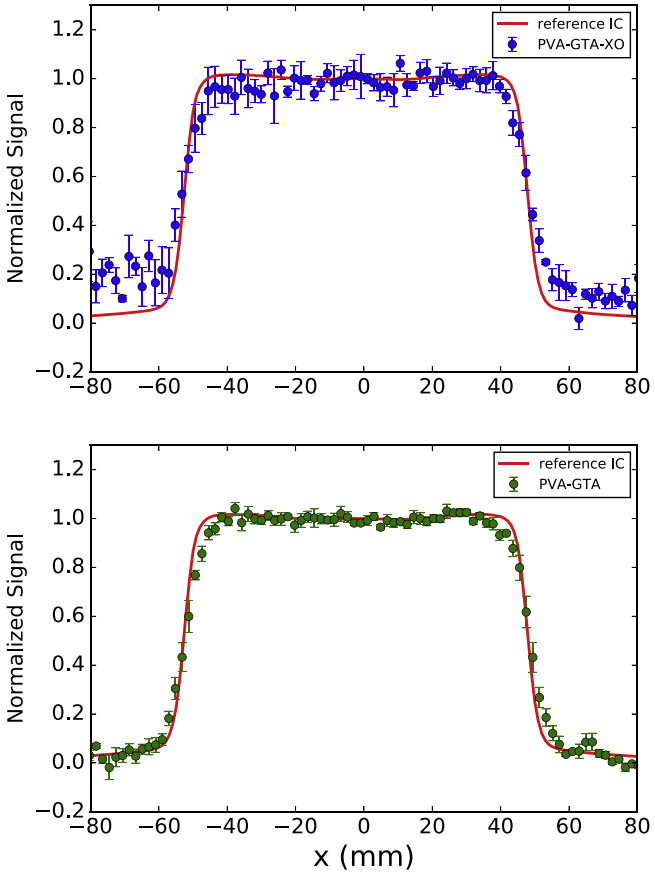

Fig. 8. Lateral dose profile obtained with PVA-GTA gels with XO (top) and without XO (bottom). Error bars correspond to 1 S.D. For comparison, the reference lateral dose profile obtained with the ionization chamber is shown as a red solid line.

Please cite this article in press as: G. Collura et al., Analysis of the response of PVA-GTA Fricke-gel dosimeters with clinical magnetic resonance imaging, Nucl. Instr. Meth. B (2017), http://dx.doi.org/10.1016/j.nimb.2017.06.012

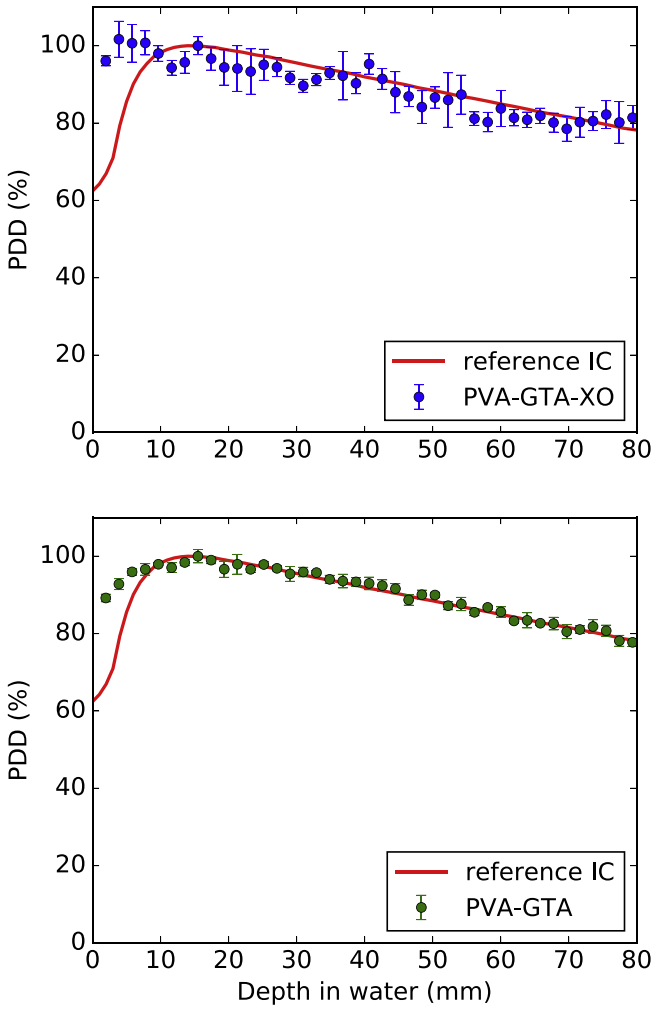

Fig. 9. Percentage depth dose (PDD) profile obtained by means of PVA-GTA gels with XO (top) and without XO (bottom). Error bars correspond to 1 S.D. For comparison the reference PDD profile obtained from the ionization chamber is reported as a solid red line.

diffusion characteristics. However both gels were found to reproduce the dose gradients they were exposed to. These gradients, in the buildup region and on the sides of the transversal profiles, were extremely steep: variations were in the order of 10%/mm, compared to a typical dose fall-off below 5 %/mm encountered in conformational radiotherapy treatments with IMRT or with the Cyberknife [77]. In fact, the gradients were so steep that even our thimble ionization chamber, with an inner diameter of 5 mm, produced results affected by volume averaging.

4. Conclusions

In this work, we investigated the MRI sensitivity of Fricke gels produced using a matrix of polyvinylalcohol cross-linked with glutaraldehyde. Having optimized the MRI acquisition parameters for these PVA-GTA gels, we found that they present good linearity of the dose response in the clinical range of 0–10 Gy and good stability of the MRI signal for several hours after irradiation. The sensitivity was found to be higher by about 40% compared to that of Fricke gels produced with agarose. In addition, PVA-GTA gel dosimeters produced without XO were found to be more sensitive to X-rays than those made with XO. Therefore, although the presence of XO allows optical imaging and can reduce the diffusion of ferric ions, its use may not always be optimal for MR imaging.

The MRI analysis of cylindrical rods of gels allowed us to evaluate the accuracy of one-dimensional dose profiles acquired with our dosimeters. PVA-GTA dosimetric gels produced without XO were found to be more precise and accurate than dosimeters with XO, as shown by a comparison against dose measurements with an ionization chamber. Our test conditions were quite demanding, with very steep dose gradients compared to actual clinical situations; nevertheless, it is clear that diffusion effects hinder accurate measurements in the dose gradient regions and they should be further reduced by modifying the gel matrix and/or by minimizing the delay between irradiation and imaging.

Acknowledgments

This research was supported in part by Grant PRIN2010SNALEM: "Development and application of new materials for ionizing radiation dosimetry" of the Italian Ministry of Education, University and Research (P.I. F. d'Errico), by Grant "NextMR" of the Italian Nuclear Physics Institute (local P.I. M. Marrale) and by Grant 2012-ATE-0392 of the University di Palermo. The authors wish to acknowledge Michele Quartararo, Marcello Mirabello and Marco Spanó for technical support, Vittorio Caputo, Chief of the Medical Physics Department of the A.O. ARNAS-Civico in Palermo, for the irradiations, and Giuseppe La Tona, Azienda Ospedaliera Universitaria Policlinico di Palermo, for MRI scans. This work was part of the post-graduate medical physics specialization thesis of Giorgio Collura.

References

[1] T. Kron, J. Lehmann, P.B. Greer, Dosimetry of ionising radiation in modern radiation oncology, Phys. Med. Biol. 61 (14) (2016) R167.
[2] J. Seco, B. Clasie, M. Partridge, Review on the characteristics of radiation detectors for dosimetry and imaging, Phys. Med. Biol. 59 (20) (2014) R303.
[3] K. Petersson, M. Jaccard, J.-F. Germond, T. Buchillier, F. Bochud, J. Bourhis, M.-C. Vozenin, C. Bailat, High dose-per-pulse electron beam dosimetry – a model to correct for the ion recombination in the Advanced Markus ionization chamber, Med. Phys. 44 (3) (2017) 1157–1167.
[4] B. Poppe, A. Djouguela, A. Blechschmidt, K. Willborn, A. Rühmann, D. Harder, Spatial resolution of 2D ionization chamber arrays for IMRT dose verification: single-detector size and sampling step width, Phys. Med. Biol. 52 (10) (2007) 2921.
[5] F. Schirru, K. Kisielewicz, T. Nowak, B. Marczewska, Single crystal diamond detector for radiotherapy, J. Phys. D 43 (26) (2010) 265101.
[6] M. Bucciolini, F.B. Buonamici, S. Mazzocchi, C. De Angelis, S. Onori, G. Cirrone, Diamond detector versus silicon diode and ion chamber in photon beams of different energy and field size, Med. Phys. 30 (8) (2003) 2149–2154.
[7] F. Oliveira, L. Amaral, A. Costa, T. Netto, Treatment verification and in vivo dosimetry for total body irradiation using thermoluminescent and semiconductor detectors, Radiat. Meas. 71 (2014) 374–378.
[8] F. Bisello, D. Menichelli, M. Scaringella, C. Talamonti, M. Zani, M. Bucciolini, M. Bruzzi, Development of silicon monolithic arrays for dosimetry in external beam radiotherapy, Nucl. Instr. Meth. Phys. Res. Sect. A 796 (2015) 85–88.
[9] M. Marrale, M. Brai, A. Triolo, A. Bartolotta, M. D'Oca, Power saturation of ESR signal in ammonium tartrate exposed to ^{60}Coγ-ray photons, electrons and protons, Radiat. Res. 166 (5) (2006) 802–809.
[10] K. Alzimami, A.M. Maghraby, D. Bradley, Comparative study of some new EPR dosimeters, Radiat. Phys. Chem. 95 (2014) 109–112.
[11] A. Wieser, F. Darroudi, EPRBioDose 2013: EPR applications and biological dosimetry, Radiat. Environ. Biophys. 53 (2) (2014) 217–220.
[12] M. Brai, G. Gennaro, M. Marrale, L. Tranchina, A. Bartolotta, M. D'Oca, ESR response to ^{60}Co-rays of ammonium tartrate pellets using Gd_2O_3 as additive, Radiat. Meas. 42 (2) (2007) 225–231.
[13] M. Brai, G. Gennaro, M. Marrale, A. Bartolotta, M. D'Oca, ESR response to γ-rays of alanine pellets containing $B(OH)_3$ or Gd_2O_3, Appl. Radiat. Isot. 65 (4) (2007) 435–439.
[14] H. Tuner, M. Kaykç, Dosimetric and kinetic investigations of γ-irradiated sodium tartrate dihydrate, Radiat. Environ. Biophys. 51 (1) (2012) 61–67.
[15] M. Marrale, M. Brai, G. Gennaro, A. Triolo, A. Bartolotta, Improvement of the LET sensitivity in ESR dosimetry for γ-photons and thermal neutrons through gadolinium addition, Radiat. Meas. 42 (6–7) (2007) 1217–1221.
[16] A. Maghraby, A. Mansour, E. Tarek, Taurine for EPR dosimetry, Radiat. Environ. Biophys. 51 (3) (2012) 255–261.
[17] S. Gallo, G. Iacoviello, A. Bartolotta, D. Dondi, S. Panzeca, M. Marrale, ESR dosimeter material properties of phenols compound exposed to radiotherapeutic electron beams, Nucl. Instr. Meth. Phys. Res. Sect. B. http://dx.doi.org/10.1016/j.nimb.2017.06.004.

Please cite this article in press as: G. Collura et al., Analysis of the response of PVA-GTA Fricke-gel dosimeters with clinical magnetic resonance imaging, Nucl. Instr. Meth. B (2017), http://dx.doi.org/10.1016/j.nimb.2017.06.012

[18] M. Marrale, M. Brai, G. Gennaro, A. Bartolotta, M. D'Oca, The effect of gadolinium on the ESR response of alanine and ammonium tartrate exposed to thermal neutrons, Radiat. Res. 169 (2) (2008) 232–239.
[19] M. Marrale, A. Longo, M. D'Oca, A. Bartolotta, M. Brai, Watch glasses exposed to 6 MV photons and 10 MeV electrons analysed by means of ESR technique: a preliminary study, Radiat. Meas. 46 (9) (2011) 822–826.
[20] O. Baffa, A. Kinoshita, Clinical applications of alanine/electron spin resonance dosimetry, Radiat. Environ. Biophys. 53 (2) (2014) 233–240.
[21] M. Marrale, A. Longo, M. Span, A. Bartolotta, M. D'Oca, M. Brai, Sensitivity of alanine dosimeters with gadolinium exposed to 6 MV photons at clinical doses, Radiat. Res. 176 (6) (2011) 821–826.
[22] M. Marrale, M. Brai, A. Longo, S. Panzeca, L. Tranchina, E. Tomarchio, A. Parlato, A. Buttafava, D. Dondi, Neutron ESR dosimetry through ammonium tartrate with low Gd content, Radiat. Protect. Dosimetry 159 (1–4) (2014) 233–236.
[23] M. Marrale, A. Longo, S. Panzeca, S. Gallo, F. Principato, E. Tomarchio, A. Parlato, A. Buttafava, D. Dondi, A. Zeffiro, ESR response of phenol compounds for dosimetry of gamma photon beams, Nucl. Instr. Meth. Phys. Res. Sect. B 339 (2014) 15–19.
[24] M. Marrale, A. Longo, G. Russo, C. Casarino, G. Candiano, S. Gallo, A. Carlino, M. Brai, Dosimetry for electron intra-operative radiotherapy: comparison of output factors obtained through alanine/epr pellets, ionization chamber and monte carlo-geant4 simulations for iort mobile dedicate accelerator, Nucl. Instr. Meth. Phys. Res. Sect. B 358 (2015) 52–58.
[25] M. Marrale, S. Gallo, A. Longo, S. Panzeca, A. Parlato, A. Buttafava, D. Dondi, A. Zeffiro, Study of the response of phenol compounds exposed to thermal neutrons beams for Electron Paramagnetic Resonance dosimetry, Radiat. Meas. 75 (2015) 15–20.
[26] S. Gallo, S. Panzeca, A. Longo, S. Altieri, A. Bentivoglio, D. Dondi, R. Marconi, N. Protti, A. Zeffiro, M. Marrale, Testing and linearity calibration of films of phenol compounds exposed to thermal neutron field for epr dosimetry, Appl. Radiat. Isot. 106 (2015) 129–133.
[27] M. Marrale, S. Basile, M. Brai, A. Longo, Monte Carlo simulation of the response of ESR dosimeters added with gadolinium exposed to thermal, epithermal and fast neutrons, Appl. Radiat. Isot. 67 (7–8 SUPPL.) (2009) 186–189.
[28] M. Marrale, A. Longo, M. Brai, A. Barbon, M. Brustolon, P. Fattibene, Pulsed EPR analysis of tooth enamel samples exposed to UV and γ-radiations, Radiat. Meas. 46 (9) (2011) 789–792.
[29] P. Fattibene, F. Trompier, A. Wieser, M. Brai, B. Ciesielski, C. De Angelis, S. Della Monaca, T. Garcia, H. Gustafsson, E.O. Hole, et al., Epr dosimetry intercomparison using smart phone touch screen glass, Radiat. Environ. Biophys. 53 (2) (2014) 311–320.
[30] A. Parlato, E. Calderaro, A. Bartolotta, M. D'Oca, M. Brai, M. Marrale, L. Tranchina, Application of the ESR spectroscopy to estimate the original dose in irradiated chicken bone, Radiat. Phys. Chem. 76 (8) (2007) 1466–1469.
[31] M. Marrale, L. Abbene, F. d'Errico, S. Gallo, A. Longo, S. Panzeca, L. Tana, L. Tranchina, F. Principato, Characterization of the ESR response of alanine dosimeters to low-energy Cu-target X-tube photons, In Press on Radiation Measurements. http://dx.doi.org/10.1016/j.radmeas.2017.03.009.
[32] A. Longo, S. Basile, M. Brai, M. Marrale, L. Tranchina, ESR response of watch glasses to proton beams, Nucl. Instr. Meth. Phys. Res. Sect. B 268 (17–18) (2010) 2712–2718.
[33] Á.B.d. Carvalho Junior, P.L. Guzzo, H.L. Sulasi, H.J. Khoury, Effect of particle size in the TL response of natural quartz sensitized by high dose of gamma radiation and heat-treatments, Mater. Res. 13 (2) (2010) 265–271.
[34] A. Triolo, M. Marrale, M. Brai, Neutron-gamma mixed field measurements by means of MCP-TLD600 dosimeter pair, Nucl. Instr. Meth. Phys. Res. Sect. B 264 (1) (2007) 183–188.
[35] A. Triolo, M. Brai, M. Marrale, G. Gennaro, A. Bartolotta, Study of the glow curves of TLD exposed to thermal neutrons, Radiat. Prot. Dosimetry. 126 (1–4) (2007) 333–336.
[36] A. Bartolotta, M. Brai, V. Caputo, M. D'Oca, A. Longo, M. Marrale, Thermoluminescence response of sodalime glass irradiated with photon and electron beams in the 1–20 Gy range, Radiat. Meas. 46 (9) (2011) 975–977.
[37] M. Marrale, A. Longo, A. Bartolotta, S. Basile, M. D'Oca, E. Tomarchio, G. Cirrone, F. Di Rosa, F. Romano, G. Cuttone, M. Brai, Thermoluminescence response of sodalime glass irradiated with proton and neutron beams, Nucl. Instr. Meth. Phys. Res. Sect. B 292 (2012) 55–58.
[38] S. Jafari, T. Jordan, M. Hussein, D. Bradley, C. Clark, A. Nisbet, N. Spyrou, Energy response of glass bead TLDs irradiated with radiation therapy beams, Radiat. Phys. Chem. 104 (2014) 208–211.
[39] M. D'Oca, A. Bartolotta, M. Cammilleri, M. Brai, M. Marrale, A. Triolo, A. Parlato, Qualitative and quantitative thermoluminescence analysis on irradiated oregano, Food Control 18 (8) (2007) 996–1001.
[40] I. Veronese, A. Galli, M.C. Cantone, M. Martini, F. Vernizzi, G. Guzzi, Study of TSL and OSL properties of dental ceramics for accidental dosimetry applications, Radiat. Meas. 45 (1) (2010) 35–41.
[41] N. Chiodini, A. Vedda, M. Fasoli, F. Moretti, A. Lauria, M.C. Cantone, I. Veronese, G. Tosi, M. Brambilla, B. Cannillo, et al., Ce-doped SiO2 optical fibers for remote radiation sensing and measurement, in: SPIE Defense, Security, and Sensing, International Society for Optics and Photonics, 2009, pp. 731616–731616.
[42] I. Veronese, C. De Mattia, M. Fasoli, N. Chiodini, E. Mones, M.C. Cantone, A. Vedda, Infrared luminescence for real time ionizing radiation detection, Appl. Phys. Lett. 105 (6) (2014) 061103.
[43] I. Veronese, N. Chiodini, S. Cialdi, E. D'Ippolito, M. Fasoli, S. Gallo, S. La Torre, E. Mones, A. Vedda, G. Loi, Real-time dosimetry with yb-doped silica optical fibres, Phys. Med. Biol. 62 (3) (2017) 4218–4236.
[44] S. Babic, J. Battista, K. Jordan, Radiochromic leuco dye micelle hydrogels: II. Low diffusion rate leuco crystal violet gel, Phys. Med. Biol. 54 (22) (2009) 6791.
[45] A. Gueli, R. De Vincolis, A. Kacperek, S. Troja, An approach to 3D dose mapping using gafchromicfilm, Radiat. Protect. Dosimetry 115 (1–4) (2005) 616–622.
[46] A. Gueli, G. Mannino, S. Troja, G. Asero, G. Burrafato, R. De Vincolis, C. Greco, N. Longhitano, A. Occhipinti, F. Pansini, et al., 3D dosimetry on Ru-106 plaque for ocular melanoma treatments, Radiat. Meas. 46 (12) (2011) 2014–2019.
[47] A.M. Gueli, N. Cavalli, R. De Vincolis, L. Raffaele, S.O. Troja, Background fog subtraction methods in gafchromicdosimetry, Radiat. Meas. 72 (2015) 44–52.
[48] M. Tamponi, R. Bona, A. Poggiu, P. Marini, A new form of the calibration curve in radiochromic dosimetry. Properties and results, Med. Phys. 43 (7) (2016) 4435–4446.
[49] A. Hiroki, Y. Sato, N. Nagasawa, A. Ohta, H. Seito, H. Yamabayashi, T. Yamamoto, M. Taguchi, M. Tamada, T. Kojima, Preparation of polymer gel dosimeters based on less toxic monomers and gellan gum, Phys. Med. Biol. 58 (20) (2013) 7131.
[50] Y. Soliman, Gamma-radiation induced synthesis of silver nanoparticles in gelatin and its application for radiotherapy dose measurements, Radiat. Phys. Chem. 102 (2014) 60–67.
[51] L. Schreiner, Review of Fricke gel dosimeters, in: Journal of Physics: Conference Series, vol. 3, IOP Publishing, 2004, pp. 9–21.
[52] J. Davies, C. Baldock, Sensitivity and stability of the Fricke-gelatin-xylenol orange gel dosimeter, Radiat. Phys. Chem. 77 (6) (2008) 690–696.
[53] M. Abdelgawad, Y. Soliman, M. El Gohry, A.A. Eldib, C.-M. Ma, O. Desouky, Measurements of radiotherapy dosimetric parameters using Fricke gel dosimeter, Biomed. Phys. Eng. Express 3 (2) (2017) 025021.
[54] L.S. Del Lama, P.C.D. Petchevist, A. de Almeida, Fricke Xylenol Gel characterization at megavoltage radiation energy, Nucl. Instrum. Methods Phys. Res., Sect. B 394 (2017) 89–96.
[55] H. Fricke, E.J. Hart, Chemical dosimetry, Radiat. Dosimetry 2 (1966) 167–239.
[56] A. Galante, H. Cervantes, C. Cavinato, L. Campos, S. Rabbani, MRI study of radiation effect on Fricke gel solutions, Radiat. Meas. 43 (2) (2008) 550–553.
[57] S. Babic, A. McNiven, J. Battista, K. Jordan, Three-dimensional dosimetry of small megavoltage radiation fields using radiochromic gels and optical CT scanning, Phys. Med. Biol. 54 (8) (2009) 2463.
[58] P. Keall, C. Baldock, A theoretical study of the radiological properties and water equivalence of Fricke and polymer gels used for radiation dosimetry, Australasian physical & engineering sciences in medicine/supported by the Australasian College of Physical Scientists in Medicine and the Australasian Association of Physical Sciences in Medicine 22 (3) (1999) 85–91.
[59] M. Bero, W. Gilboy, P. Glover, H. El-Masri, Tissue-equivalent gel for non-invasive spatial radiation dose measurements, Nucl. Instrum. Methods Phys. Res. Sect. B 166 (2000) 820–825.
[60] G. Gambarini, I. Veronese, L. Bettinelli, M. Felisi, M. Gargano, N. Ludwig, C. Lenardi, M. Carrara, G. Collura, S. Gallo, et al., Study of optical absorbance and MR relaxation of Fricke xylenol orange gel dosimeters, In Press on Radiation Measurements. http://dx.doi.org/10.1016/j.radmeas.2017.03.024.
[61] Y.S. Soliman, M. El Gohary, M.A. Gawad, E. Amin, O. Desouky, Fricke gel dosimeter as a tool in quality assurance of the radiotherapy treatment plans, Appl. Radiat. Isot. 120 (2017) 126–132.
[62] G. Gambarini, C. Birattari, M. Mariani, R. Marchesini, L. Pirola, P. Prestini, M. Sella, S. Tomatis, Study of light transmittance from layers of Fricke-xylenol-orange-gel dosimeters, Nucl. Instrum. Methods Phys. Res. Sect. B 213 (2004) 321–324.
[63] J. Gore, Y. Kang, Measurement of radiation dose distributions by nuclear magnetic resonance (NMR) imaging, Phys. Med. Biol. 29 (10) (1984) 1189.
[64] S. Di Capua, F. d'Errico, E. Egger, L. Guidoni, A.M. Luciani, A. Rosi, V. Viti, Dose distribution of proton beams with NMR measurements of Fricke-agarose gels, Magn. Resonance Imaging 15 (4) (1997) 489–495.
[65] M. Marrale, M. Brai, C. Gagliardo, S. Gallo, A. Longo, L. Tranchina, B. Abbate, G. Collura, K. Gallias, V. Caputo, A. Lo Casto, M. Midiri, F. d'Errico, Correlation between ferrous ammonium sulfate concentration, sensitivity and stability of Fricke gel dosimeters exposed to clinical X-ray beams, Nucl. Instrum. Methods Phys. Res. Sect. B 335 (2014) 54–60.
[66] M. Marrale, M. Brai, A. Longo, S. Gallo, E. Tomarchio, L. Tranchina, C. Gagliardo, F. d'Errico, MR relaxometry measurements of Fricke gel dosimeters exposed to neutrons, Radiat. Phys. Chem. 104 (4) (2014) 424–428.
[67] R. Schulz, D. Nguyen, J. Gore, et al., Dose-response curves for Fricke-infused agarose gels as obtained by nuclear magnetic resonance, Phys. Med. Biol. 35 (12) (1990) 1611.
[68] W.I. Rae, C.A. Willemse, M.G. Lötter, J.S. Engelbrecht, J.C. Swarts, Chelator effect on ion diffusion in ferrous-sulfate-doped gelatin gel dosimeters as analyzed by MRI, Med. Phys. 23 (1) (1996) 15–23.
[69] C. Baldock, P. Harris, A. Piercy, B. Healy, Experimental determination of the diffusion coefficient in two-dimensions in ferrous sulphate gels using the finite element method, Aust. Phys. Eng. Sci. Med. 24 (1) (2001) 19–30.
[70] B. Hill, S.Å.J. Bäck, M. Lepage, J. Simpson, B. Healy, C. Baldock, Investigation and analysis of ferrous sulfate polyvinyl alcohol (PVA) gel dosimeter, Phys. Med. Biol. 47 (23) (2002) 4233.
[71] K. Chu, K. Jordan, J. Battista, J. Van Dyk, B. Rutt, Polyvinyl alcohol-Fricke hydrogel and cryogel: two new gel dosimetry systems with low $Fe^{3}+$ diffusion, Phys. Med. Biol. 45 (4) (2000) 955.

Please cite this article in press as: G. Collura et al., Analysis of the response of PVA-GTA Fricke-gel dosimeters with clinical magnetic resonance imaging, Nucl. Instr. Meth. B (2017), http://dx.doi.org/10.1016/j.nimb.2017.06.012

[72] F. d'Errico, L. Lazzeri, D. Dondi, M. Mariani, M. Marrale, G. Gambarini, Novel GTA-PVA Fricke gels for three-dimensional dose mapping in radiotherapy, In press on Radiation Measurements.
[73] A. Marini, L. Lazzeri, M. Cascone, R. Ciolini, L. Tana, F. d'Errico, Fricke gel dosimeters with low-diffusion and high-sensitivity based on a chemically cross-linked PVA matrix, In Press on Radiation Measurements. http://dx.doi.org/10.1016/j.radmeas.2017.02.012.
[74] M. Marrale, G. Collura, S. Gallo, S. Nici, L. Tranchina, B.F. Abbate, S. Marineo, S. Caracappa, F. d'Errico, Analysis of spatial diffusion of ferric ions in PVA-GTA gel dosimeters through magnetic resonance imaging, Nucl. Instr. Meth. Phys. Res. Sect. B 396 (2017) 50–55.
[75] B. Healy, M. Zahmatkesh, K. Nitschke, C. Baldock, Effect of saccharide additives on response of ferrous–agarose–xylenol orange radiotherapy gel dosimeters, Med. Phys. 30 (9) (2003) 2282–2291.
[76] P. Andreo, M.S. Huq, M. Westermark, H. Song, A. Tilikidis, L. DeWerd, K. Shortt, Protocols for the dosimetry of high-energy photon and electron beams: a comparison of the IAEA TRS-398 and previous international Codes of Practice, Phys. Med. Biol. 47 (17) (2002) 3033.
[77] S. Hossain, P. Xia, K. Huang, M. Descovich, C. Chuang, A.R. Gottschalk, M.R.L. Ma III, Dose Gradient Near Target Normal Structure Interface for Nonisocentric Cyber Knife and Isocentric Intensity-Modulated Body Radiotherapy for Prostate Cancer, Int. J. Radiat. Oncol. Biol. Phys. 78 (1) (2010) 58–63.

Please cite this article in press as: G. Collura et al., Analysis of the response of PVA-GTA Fricke-gel dosimeters with clinical magnetic resonance imaging, Nucl. Instr. Meth. B (2017), http://dx.doi.org/10.1016/j.nimb.2017.06.012